学会発表：

招待講演

1 浅原弘嗣．システムアプローチによる運動器発生メカニズムの解明．第 23 回日本軟骨代謝学会；ランチョンセミナー2，鹿児島．4 月 2～3 日，2010.
2 Asahara H. A systems approach reveals that the myogenesis genome network is regulated by the transcriptional repressor RP58. 2nd Joint Meeting of the French and Japanese Societies for Developmental Biology; Session 3"Cell Fate Specification and Gene Regulatory Networks" Oral Presentation 17, Paris, France. May 26-28, 2010.
3 浅原弘嗣．miRNA による軟骨の発生と疾患ネットワークの解明．第 4 回 骨・軟骨フロンティア，東京．11 月 20 日，2010.

シンポジウム

1. 浅原弘嗣．システムアプローチによる運動器疾患の解明．日本ヒトプロテオーム機構第 8 回大会（日本プロテオーム学会 2010 年会） 第 6 回日本臨床プロテオーム研究会；シンポジウム 5 (S5)「先端技術」S5-3，千葉．7 月 26～27 日，2010.
2. 浅原弘嗣．システムアプローチによる運動器の発生と疾患の解析．第 19 回硬組織再生生物学会学術大会；シンポジウム「リウマチ・軟骨治療の分子基盤」S-4，岡山．9 月 4 日，2010.
3. 浅原弘嗣．システム研究による運動器の発生メカニズムの解明と医療への応用．第 51 回日本組織細胞化学会総会・学術集会；シンポジウム 2「発生・生殖生物学の最前線」S2-04，東京．9 月 4～5 日，2010.

一般演題発表

1. Asahara H. Micro-RNA-140 plays dual roles both in cartilage development and homeostasis. The 19th CDB Meeting "RNA Sciences in Cell and Developmental Biology"; Poster Introduction 1 & Poster Session 1, Hyogo, Japan. May 10-12, 2010.
2. Yokoyama S, Ito Y, Asahara H. Systems approach revealed novel myogenic transcriptional network regulated by RP58. 第 43 回日本発生生物学会；Hot Topics 2 & Poster，京都．6 月 20～23 日，2010.
3. Miyaki S, Sato T, Inoue S, Otsuki S, Ito Y, Yokoyama S, Kato Y, Yamashita S, Nakasa T, Lotz MK, Kudo-Ueno H, Asahara H. Cartilage-specific microRNA-140 regulates tissue homeostasis and protects against osteoarthritis-like pathology. OARSI 2010 World Congress on Osteoarthritis; Concurrent Session 10: Genetics, Genomics and Epigenetics 67, Brussels, Belgium. September 23-26, 2010.
4. Ito Y, Yokoyama S, Asahara H. Development of locomotive tissue complex organized by RP58:Mkx. EXCITING BIOLOGIES: Biology of Recognition; Poster Session, Sentosa Island, Singapore. October 7-9, 2010.
5. Sato T, Miyaki S, Inoue A, Otsuki S, Ito Y, Yokoyama S, Kato Y, Nakasa T, Yamashita S, Takada S, Lotz MK, Asahara H. MicroRNA-140 plays dual roles in both cartilage development and homeostasis. 第 33 回 日本分子生物学会年会 第 83 回 日本生化学会大会 合同大会；一般演題（ポスター）「10 疾患生物学 5) 老化と生活習慣病」3P-1103，兵庫．12 月 7～10 日，2010.
6. 関敦仁，高山真一郎，細見僚，斎藤治和，森澤妥．Madelug 変形に対する矯正骨切り術の工夫．第 53 回日本手の外科学会学術集会，新潟．4 月 15～17 日，2010.
7. Seki A, Takagi T, Morisawa Y, Miyazaki K, Sasaki K, Takayama S. A new osteoromy for Madelung deformity. 11th Triennial Congress of the International Federation of Society of the Hand, Seoul, Korea, South. October 31-November 4, 2010.

8. 関敦仁，高山真一郎，日下部浩，高木岳彦，宮崎馨，佐々木康介．肥厚性皮膚骨膜症の関節症状に関する文献的考察．第 21 回日本小児整形外科学会，徳島．11 月 26～27 日，2010.

V. 研究成果の刊行物・別刷

Mod Rheumatol (2010) 20:11–17
DOI 10.1007/s10165-009-0224-7

ORIGINAL ARTICLE

Correlation between MMP-13 and HDAC7 expression in human knee osteoarthritis

Reiji Higashiyama · Shigeru Miyaki · Satoshi Yamashita · Teruhito Yoshitaka · Görel Lindman · Yoshiaki Ito · Takahisa Sasho · Kazuhisa Takahashi · Martin Lotz · Hiroshi Asahara

Received: 3 April 2009 / Accepted: 5 August 2009 / Published online: 26 September 2009

Abstract Recent studies suggest that histone deacetylase (HDAC) inhibitors may therapeutically prevent cartilage degradation in osteoarthritis (OA). Matrix metalloproteinase-13 (MMP-13) plays an important role in the pathogenesis of this disease and in the present study we investigated the correlation between HDACs and MMP-13. Comparing the expression of different HDACs in cartilage from OA patients and healthy donors, HDAC7 showed a significant elevation in cartilage from OA patients. High level of HDAC7 expression in OA cartilage was also confirmed by immunohistochemistry. Knockdown of HDAC7 by small interference RNA (siRNA) in SW1353 human chondrosarcoma cells strongly suppressed interleukin (IL)-1-dependent and independent induction of MMP-13 gene expression. In conclusion, elevated HDAC7 expression in human OA may contribute to cartilage degradation via promoting MMP-13 gene expression, suggesting the critical role of MMP-13 in OA pathogenesis.

Keywords Osteoarthritis · HDAC7 and MMP-13

R. Higashiyama · S. Miyaki · M. Lotz · H. Asahara
Division of Arthritis Research, The Scripps Research Institute, 10550 North Torrey Pines Road, La Jolla, CA 92037, USA

R. Higashiyama · S. Yamashita · T. Yoshitaka · G. Lindman · Y. Ito · H. Asahara (✉)
Department of Systems BioMedicine, National Research Institute for Child Health and Development, 2-10-1 Okura, Setagaya, Tokyo 157-8535, Japan
e-mail: asahara@nch.go.jp

R. Higashiyama · T. Sasho · K. Takahashi
Department of Orthopaedic Surgery, Graduate School of Medicine, Chiba University, Chiba, Japan

Abbreviations

MMP	Matrix metalloproteinase
OA	Osteoarthritis
HDAC	Histone deacetylase
RT-PCR	Reverse-transcriptase polymerase chain reaction
IL-1	Interleukin-1β
TSA	Trichostatin A

Background

Osteoarthritis (OA) is a chronic degenerative joint disorder and a major cause of disability in the elderly. Characterized by progressive structural changes in articular cartilage, with persistent degeneration the disease eventually leads to loss of joint function. A significant feature of OA is excessive production of inflammatory mediators [1–3], among which pro-inflammatory cytokine interleukin-1β (IL-1) plays a crucial role in the pathophysiology. IL-1 induces a cascade of inflammatory and catabolic events in chondrocytes, changing chondrocyte anabolism through suppression of proteoglycan and collagen synthesis and by enhancing matrix metalloproteinase (MMP) production.

Several lines of evidence suggest that MMP-13 contributes to cartilage degradation in OA. MMP-13 expression is significantly higher in chondrocytes from cartilage of late-stage OA compared with early OA or normal knee cartilage [4]. In explant cultures treated with a specific MMP-13 inhibitor, release of collagen degradation products from human OA cartilage is reduced [5]. Furthermore, transgenic mice overexpressing activated MMP-13 in the articular chondrocytes develop joint degradation similar to human OA [6]. Characterization of MMP-13 expression

regulation in articular chondrocytes will contribute to understanding the molecular etiology of OA.

Two families of histone deacetylase (HDACs) have been identified: the classical HDAC family and the NAD^+-dependent, so-called SIR2 family (sometimes called class III HDACs). Classical HDACs can be grouped into 3 classes (I, II, and IV) based on phylogeny [7]. Class I HDACs (HDAC1, 2, 3, and 8) are related to yeast RPD3, and class II HDACs (HDAC4, 5, 6, 7, 9, and 10) are more closely related to yeast HDA1 [8]. HDAC11 alone represents class IV, and HDAC11-related proteins have been described in all eukaryotic organisms with the exception of fungi [7]. Trichostatin A (TSA) is a HDAC inhibitor [8] with a broad spectrum of activity against class I and II HDACs, but not HDACs from the SIR2 family. Administration of these reagents to cells blocks histone deacetylation and leads to increased histone acetylation within gene expression in susceptible genes. There are also, however, many cases in which HDAC inhibitors act as repressors of gene expression [9–13].

Recently, HDACs have emerged as targets in cancer therapy and inflammatory diseases, including rheumatoid arthritis (RA) and OA [14–23], but it is still unclear which HDACs are specifically involved in cartilage degradation. These observations prompted us to investigate HDAC expression in normal and OA cartilage and identify the specific HDAC that contributes to cartilage degradation in human OA.

Materials and methods

Cartilage procurement and processing

Cartilage was obtained from 6 normal donors (age range 19–49 years; Mankin score 0–2 points) and 10 OA donors (age range 44–93 years; Mankin score 5–10 points). All tissue samples were graded according to a modified Mankin scale [24], for which <3 points was normal and ≥5 points represented OA. Normal articular cartilage was harvested from femoral condyles and tibial plateaus of human tissue donors under approval from the Scripps Human Subjects Committee. Osteoarthritis cartilage was obtained from patients undergoing knee replacement surgery. Cartilage thickness ranged from 1.5 to 2.8 mm. Cartilage surfaces were rinsed with saline and parallel sections 5 mm apart were cut vertically from the cartilage surface onto subchondral bone with a scalpel. These cartilage strips were then resected from bone. Human chondrocytes were isolated and cultured as previously described [25]. Cartilage tissue was incubated with trypsin at 37°C for 10 min. Following removal of trypsin solution, tissue slices were treated for 12–16 h with type IV clostridial collagenase in Dulbecco's modified Eagle's medium (DMEM) with 5% fetal calf serum. After initial isolation, cells were kept in high-density cultures in DMEM (high glucose) supplemented with 10% CS, L-glutamine, and antibiotics and allowed to attach to the surface of the culture flasks. After cells had grown to confluence, they were split once (passage 1) and grown to confluence again in preparation for experiments [26].

Cell culture

Human knee chondrocytes were grown to confluence in 35-mm 6-well plates with 2 mL DMEM containing 10% CS with or without TSA (SIGMA Inc.) at 300 nM for 24 h (Fig. 1a). In parallel, cells were precultured for 5 h with 5 ng/mL IL-1, after which TSA was added at 300 nM and cultured additionally 24 h (Fig. 1b).

Knockdown experiments by small interference RNA (siRNA) were carried out on SW1353 human chondrosarcoma cells transfected with 25 nmol siHDAC7 (Applied Biosystems Inc.) using Lipofectamine 2000 (Invitrogen Corporation) for 5 h, following the manufacturer's instructions. Then incubation with 5 ng/mL IL-1 was done. In preliminary experiments, we could knock down the HDAC7 expression level to 20% by 25 nmol siHDAC7. Because the siHDAC7 effect was not enough in human

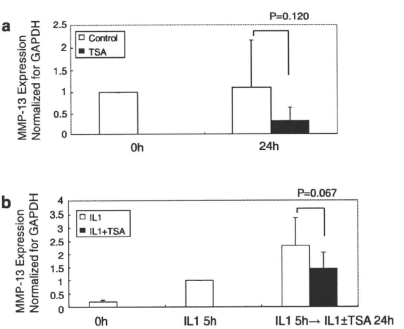

Fig. 1 TSA suppresses both natural and IL-1-induced MMP-13 expression. TSA lowered both natural and IL-1-induced MMP-13 expression, although the effect was not statistically significant. Real-time PCR results from **a** human knee chondrocytes ($n = 6$, age range 19–66 years) treated or untreated with 300 nM TSA for 24 h, and **b** chondrocytes stimulated with IL-1 (5 ng/mL) for 5 h and then treated or untreated with TSA (300 nM) for 24 h. GAPDH gene expression was used for normalization. Results are expressed as fold changes relative to a value of 1 for untreated control cells. $P = 0.120$ (**a**). Results are expressed as fold changes relative to a value of 1 for untreated control cells after 5 h of IL-1 stimulation. $P = 0.067$ (**b**)

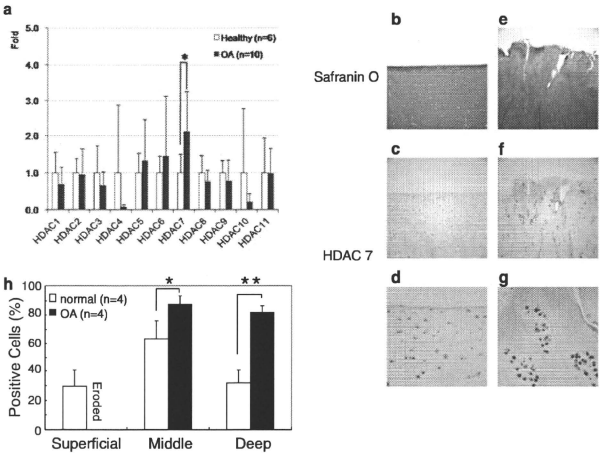

Fig. 2 Localization of HDAC7 in normal and OA knee cartilage. **a** HDAC1–11 mRNA expression in human knee cartilage was determined by real-time RT-PCR. In normal samples, HDAC3 was the most abundantly expressed HDAC (data not shown). HDAC7 had significantly higher expression in OA than in normal cartilage (Fig. 2a). Cartilage was obtained from 6 normal donors (mean age 30.8 years; range 19–49 years; Mankin score 0–2 points) and 10 OA donors (mean age 71.6 years; range 44–93 years old; Mankin score 5–10 points) (Fig. 2a). The results are expressed as mean ± SD. $^{*}P < 0.05$. **b–g** HDAC7 localization was examined in tissue from 4 normal donors (age range 19–48 years) and 4 OA donors (age range 48–93 years). HDAC7-positive cells were more frequent in OA cartilage than in normal cartilage. The immunoreactive product is *dark red*. ×10 (**b**, **c**, **e**, **f**). **h** The number of HDAC7-positive cells was counted in the superficial, middle, and deep zones of sections from normal ($n = 4$) and OA ($n = 4$) cartilage with specific antibodies. The OA middle and deep zones had significantly more HDAC7-positive cells than did normal middle and deep zones, respectively. The results are expressed as mean ± SD. $^{*}P < 0.05$, $^{**}P < 0.01$

normal chondrocytes, we used SW1353 human chondrosarcoma cells for this assay (data not shown).

Quantitative polymerase chain reaction

Total RNA was isolated from cartilage tissues or monolayer chondrocyte cultures using Trizol (Invitrogen Inc., Carlsbad, CA, USA). Complementary DNA was produced using Ready-To-Go You Prime First Strand Beads (GE Health Inc., USA) with 2 μg total RNA and oligo (dT) primers. Messenger RNA expression of HDAC1–11 and MMP-13 was detected by real-time RT-PCR with TaqMan Gene Expression Assay probe (Applied Biosystems Inc.) using an iCycler (Bio-Rad Laboratories Inc., Hercules, CA, USA) as follows: 10 min at 95°C for initial denaturation, followed by 45 cycles at 95°C (15 s) and 60°C (1 min). The expression levels of HDACs and MMP-13 were defined from the threshold cycle (Ct) and relative values were calculated by the $2^{-\Delta\Delta Ct}$ method after normalizing expression to GAPDH.

Histology and immunohistochemistry

Cartilage tissues were fixed with 4% paraformaldehyde and stained with Safranin O. HDAC7 antibodies were purchased from Santa Cruz Biotechnologies (catalog no. sc-11421, Santa Cruz, CA, USA). Paraffin-fixed samples were first deparaffinized in xylene substitute Pro-Par Clearant (Anatech Ltd, Battle Creek, MI, USA) and ethanol before rehydration in water. Following a wash with phosphate-buffered saline (PBS), sections were blocked with 0.1% Tween 20 with 3% normal goat serum for 30 min at room temperature. HDAC7 antibodies (1:50 dilution; 4 μg/mL) and normal rabbit immunoglobulin G (IgG, 4 μg/mL) as a negative control were applied and incubated overnight at 4°C. After washing with PBS, sections were incubated with biotinylated goat anti-rabbit secondary antibody for 30 min (1:200; Vector Laboratories Inc., Burlingame, CA, USA) and then incubated with Vectastain ABC-AP kit (AK-5000; Vector Laboratories Inc., Burlingame, CA, USA) for 30 min at room temperature. Finally, sections

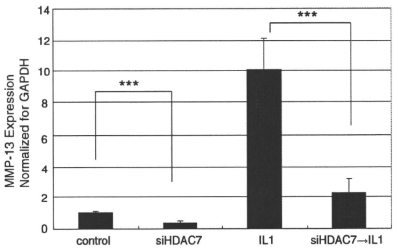

Fig. 3 Knockdown of HDAC7 by siRNA in SW1353 human chondrosarcoma cells. Real-time PCR results of MMP-13 expression in HDAC7 knocked down cells with and without the additional 5 h of culturing in IL-1 (5 ng/mL). Knockdown of HDAC7 decreased both natural and IL-1-induced MMP-13 expression. Data are presented as mean ± SD ($n = 2$, in duplicate). ***$P < 0.001$

were stained with an alkaline phosphatase substrate kit (Vector Laboratories Inc., Burlingame, CA, USA).

Quantification and localization of signals throughout cartilage

To systematically assess HDAC7 localization throughout each cartilage zone, we counted positive and negative cells in a 50 × 50 μm^2 grid (using a 40× field objective) starting from the cartilage surface to the deep zone (DZ). This procedure was repeated a minimum of 5 times for each section. We based our identification of each zone on previously reported characteristics that comprise cell shape, morphology, orientation, and pericellular matrix (PM) deposition [27]. Thus, superficial zone (SZ) cells were characterized by their elongated shape, their parallel orientation relative to the surface, and their lack of extensive PM. These cells predominate within the first 50 μm. The middle zone (MZ) was distinguishable by the presence of rounded cells without an organized orientation relative to the surface, an extracellular matrix (ECM) rich in proteoglycans, and evidence of PM. Conversely, DZ cells were recognized by extensive PM deposition and an organization of 3 or more cells in chondron groups arranged in columns. The depth of each zone was recorded for each section for comparative analysis on the frequency of positive signals in each zone. The frequency of positive cells was expressed as a percentage relative to the total number of cells counted in each zone.

Statistical analysis

Statistically significant differences between 2 groups were determined with t tests. Results are presented as mean ± standard deviation (SD). P values of less than 0.05 were considered statistically significant.

Results

Histone deacetylase inhibitor TSA modulates MMP-13 gene expression

To examine the potential role of HDACs on MMP13 expression, chondrocytes were treated with TSA, a HDAC inhibitor. We used normal chondrocytes ($n = 6$) to exclude effect of OA changes on chondrocytes. When treating human knee chondrocytes with TSA only, natural MMP-13 expression was suppressed to a small degree ($P = 0.120$) and with IL-1 induction of MMP-13 the suppression was greater ($P = 0.067$), but none of the results were statistically significant (Fig. 1). Even though not significant, these results provide a clue and increase our curiosity to which HDAC is affecting the MMP-13 expression.

HDAC7 expression is elevated in OA cartilage

All the knee cartilage samples obtained for this study were examined for HDAC1–11 messenger RNA (mRNA) expressions in human by real-time PCR. Expression of HDAC7 was significantly higher in OA than in normal cartilage (Fig. 2a). On the other hand, HDAC4 and HDAC10 were relatively lower in OA cartilage, although the changes were not statistically significant.

Normal and OA samples stained with Safranin O (Fig. 2b, e) displayed different localization of HDAC7-positive cells. In normal cartilage, we detected positive cells in the MZ (Fig. 2c), whereas in OA cartilage we detected many positive cells, especially in chondrocyte clusters (Fig. 2f, g). Representative examples were a normal 19-year-old female (Mankin score 1) and a 57-year-old male with OA (Mankin score 9). Figure 2h presents the quantitative analysis of zonal distribution of HDAC7-expressing cells in 4 normal (range 19–48 years old) and OA (range 48–93 years old) donors. Complete erosion of the SZ was observed in OA cartilage. Moreover, significantly more positive cells were observed in middle and DZs in OA cartilage, compared with in normal middle and DZs, respectively.

Knockdown of HDAC7 significantly decreases MMP-13 expression

To investigate the correlation between HDAC7 and MMP-13, HDAC7 was knocked down by siRNA in SW1353 human chondrosarcoma cells and mRNA expression of MMP-13 was measured by real-time RT-PCR. HDAC7

knockdown cells were further stimulated with IL-1, and MMP-13 expression was measured again. Knocking down HDAC7 in SW1353 cells decreased both natural and IL-1-induced MMP-13 expression significantly (Fig. 3), indicating functional interaction between HDAC7 and MMP-13.

Discussion

Onset and progression of OA is associated with changes in chondrocyte gene expression. HDACs balance histone acetyltransferases (HATs) and regulate gene transcription epigenetically, and thereby control the acetylation status of histone proteins and nonhistone substrates. In general, acetylation of histones loosens nucleosomal structures, which promotes gene transcription. In contrast, deacetylation of histones stabilizes nucleosomal structures and represses gene transcription [28, 29]. However, emerging evidence indicates that gene regulation by acetylation/deacetylation is more dynamic and complex, and that HATs also can act as repressors and HDACs as transcription activators. Indeed, global analysis of gene expression has shown that inhibition of HDAC activity results in both induction and repression of gene expression [30–35]. Recent studies demonstrated that HDAC inhibitors have therapeutic effects in cancer and inflammatory diseases [14–23]. Young et al. [22] revealed that HDAC inhibitors modulate MMP gene expression in chondrocytes and block cartilage resorption. Although we could not find a statistically significant difference, there is a tendency for MMP13 to be reduced by TSA treatment. As TSA inhibits multiple HDACs, it may be difficult to see direct effect of specific HDAC inhibition by TSA treatment. In this regard, our data showing that specific reduction of HDAC7 by siRNA inhibited MMP-13 expression (Fig. 3) support the idea that HDAC7 promotes MMP-13 in OA pathogenesis.

Matrix metalloproteinases are a family of enzymes that collectively degrade components of the ECM. They are important in normal physiological processes such as development and wound healing, where they appear in a low concentration. In contrast, aberrant MMP expression occurs in several disease states, including atherosclerosis, tumor invasion, and arthritic diseases [36, 37]. MMPs mediate irreversible matrix degradation and subsequent joint destruction in RA and OA. MMP-13 is expressed by chondrocytes and is critical for collagen degradation as it hydrolyzes type II collagen more efficiently than do other collagenases [38]. Therefore, we wanted to see whether a specific HDAC is responsible for IL-1-induced MMP-13 expression and thus contributes to cartilage degradation in OA.

In the present study, we observed significant upregulation of HDAC7 in OA cartilage by real-time RT-PCR and immunohistochemistry (Fig. 2a). HDAC7 is a member of the class II HDACs, which comprises HDAC4, 5, 6, 7, 9, and 10, all of which display cell-type-restricted patterns of expression and contain a highly conserved C-terminal deacetylase catalytic domain. Class II HDACs also contain an N-terminal extension that links them to specific transcription factors and confers responsiveness to a variety of signal transduction pathways serving as a link between the genome and the extracellular environment [39]. Disruption of the HDAC7 gene in mice results in embryonic lethality due to a failure of endothelial cell–cell adhesion and consequent dilatation and rupture of blood vessels. HDAC7 represses MMP-10 gene transcription by associating with myocyte enhancer factor-2 (MEF2), a direct activator of MMP-10 transcription and an essential regulator of angiogenesis [40].

Recently, Jensen et al. [41] demonstrated that HDAC7 associates with Runx2 and represses its activity during osteoblast maturation. Runx2 is required for MMP-13 promoter activity induced by IL-1 [42]. Increased expression of Runx2 in OA cartilage may contribute to increased expression of MMP-13 [43]. Kawaguchi [44] proposed that endochondral ossification signals, in which Runx2 plays a central role, may be important for OA progression [45]. The expression pattern of HDAC7 is different between normal and OA cartilage and the localization of HDAC7 in OA is similar to Runc2 expression in OA [43], suggesting the potential link between Runx2 and HDAC7 in OA pathogenesis. It will be interesting to test whether HDAC7 and Runx2 may cooperatively regulate MMP13 in chondrocytes.

The human genome contains only 18 HDAC genes, but more than 1,800 genes are predicted to encode transcription factors [46]. Given the number of other mechanisms for regulation of MMP-13 expression [47–53], it is important to identify the precise mechanism for how HDAC7 may regulate MMP-13 via specific transcription factors in OA chondrocytes. On the other hand, it is likely that HDAC7 regulates many other OA-related genes. Based on our current study showing the link between HDAC7 and MMP-13 in OA chondrocytes, it is important to examine other HDAC7 targets in OA pathogenesis and test whether HDAC7 could be a therapeutic target by in vivo study.

Conclusions

Our findings support the idea that HDAC7 expression is elevated in human OA cartilage and promotes IL-1 induction of MMP13, contributing to cartilage degradation. Many enigmatic interactions remain unclear, and further

studies are needed to elucidate the mechanism of cartilage degradation by MMP-13 in OA.

Acknowledgments This study was supported by NIH grants AR056120, AR050631, AG007996, and AG033409.

Conflict of interest statement None.

References

1. Pelletier JP, Martel-Pelletier J, Abramson SB. Osteoarthritis, an inflammatory disease: potential implication for the selection of new therapeutic targets. Arthritis Rheum. 2001;44(6):1237–47.
2. Goldring MB. The role of the chondrocyte in osteoarthritis. Arthritis Rheum. 2000;43(9):1916–26.
3. Goldring MB, Berenbaum F. The regulation of chondrocyte function by proinflammatory mediators prostaglandins and nitric oxide. Clin Orthop Relat Res. 2004;427(suppl):S37–46.
4. Bau B, Gebhard PM, Haag J, Knorr T, Bartnik E, Aigner T. Relative messenger RNA expression profiling of collagenases and aggrecanases in human articular chondrocytes in vivo and in vitro. Arthritis Rheum. 2002;46(10):2648–57.
5. Billinghurst RC, Dahlberg L, Ionescu M, Reiner A, Bourne R, Rorabeck C, et al. Enhanced cleavage of type II collagen by collagenases in osteoarthritic articular cartilage. J Clin Invest. 1997;99(7):1534–45.
6. Neuhold LA, Killar L, Zhao W, Sung ML, Warner L, Kulik J, et al. Postnatal expression in hyaline cartilage of constitutively active human collagenase-3 (MMP-13) induces osteoarthritis in mice. J Clin Invest. 2001;107(1):35–44.
7. Gregoretti IV, Lee YM, Goodson HV. Molecular evolution of the histone deacetylase family: functional implications of phylogenetic analysis. J Mol Biol. 2004;338(1):17–31.
8. de Ruijter AJ, van Gennip AH, Caron HN, Kemp S, van Kuilenburg AB. Histone deacetylases (HDACs): characterization of the classical HDAC family. Biochem J. 2003;370(Pt 3):737–49.
9. Bernstein BE, Tong JK, Schreiber SL. Genomewide studies of histone deacetylase function in yeast. Proc Natl Acad Sci USA. 2000;97(25):13708–13.
10. Mulholland NM, Soeth E, Smith CL. Inhibition of MMTV transcription by HDAC inhibitors occurs independent of changes in chromatin remodeling and increased histone acetylation. Oncogene. 2003;22(31):4807–18.
11. Nair AR, Boersma LJ, Schiltz L, Chaudhry MA, Muschel RJ. Paradoxical effects of trichostatin A: inhibition of NF-Y-associated histone acetyltransferase activity, phosphorylation of hGCN5 and downregulation of cyclin A and B1 mRNA. Cancer Lett. 2001;166(1):55–64.
12. Pujuguet P, Radisky D, Levy D, Lacza C, Bissell MJ. Trichostatin A inhibits beta-casein expression in mammary epithelial cells. J Cell Biochem. 2001;83(4):660–70.
13. Saunders N, Dicker A, Popa C, Jones S, Dahler A. Histone deacetylase inhibitors as potential anti-skin cancer agents. Cancer Res. 1999;59(2):399–404.
14. Lin HY, Chen CS, Lin SP, Weng JR. Targeting histone deacetylase in cancer therapy. Med Res Rev. 2006;26(4):397–413.
15. Villar-Garea A, Esteller M. Histone deacetylase inhibitors: understanding a new wave of anticancer agents. Int J Cancer. 2004;112(2):171–8.
16. Johnstone RW. Histone-deacetylase inhibitors: novel drugs for the treatment of cancer. Nat Rev Drug Discov. 2002;1(4):287–99.
17. Kortenhorst MS, Carducci MA, Shabbeer S. Acetylation and histone deacetylase inhibitors in cancer. Cell Oncol. 2006;28(5–6):191–222.
18. Blanchard F, Chipoy C. Histone deacetylase inhibitors: new drugs for the treatment of inflammatory diseases? Drug Discov Today. 2005;10(3):197–204.
19. Lin HS, Hu CY, Chan HY, Liew YY, Huang HP, Lepescheux L, et al. Anti-rheumatic activities of histone deacetylase (HDAC) inhibitors in vivo in collagen-induced arthritis in rodents. Br J Pharmacol. 2007;150(7):862–72.
20. Nasu Y, Nishida K, Miyazawa S, Komiyama T, Kadota Y, Abe N, et al. Trichostatin A, a histone deacetylase inhibitor, suppresses synovial inflammation and subsequent cartilage destruction in a collagen antibody-induced arthritis mouse model. Osteoarthr Cartil. 2008;16(6):723–32.
21. Nishida K, Komiyama T, Miyazawa S, Shen ZN, Furumatsu T, Doi H, et al. Histone deacetylase inhibitor suppression of autoantibody-mediated arthritis in mice via regulation of p16INK4a and p21(WAF1/Cip1) expression. Arthritis Rheum. 2004;50(10):3365–76.
22. Young DA, Lakey RL, Pennington CJ, Jones D, Kevorkian L, Edwards DR, et al. Histone deacetylase inhibitors modulate metalloproteinase gene expression in chondrocytes and block cartilage resorption. Arthritis Res Ther. 2005;7(3):R503–12.
23. Chabane N, Zayed N, Afif H, Mfuna-Endam L, Benderdour M, Boileau C, et al. Histone deacetylase inhibitors suppress interleukin-1beta-induced nitric oxide and prostaglandin E2 production in human chondrocytes. Osteoarthr Cartil. 2008;16(10):1267–74.
24. Thomas CM, Fuller CJ, Whittles CE, Sharif M. Chondrocyte death by apoptosis is associated with cartilage matrix degradation. Osteoarthr Cartil. 2007;15(1):27–34.
25. Blanco FJ, Ochs RL, Schwarz H, Lotz M. Chondrocyte apoptosis induced by nitric oxide. Am J Pathol. 1995;146(1):75–85.
26. Otsuki S, Taniguchi N, Grogan SP, D'Lima D, Kinoshita M, Lotz M. Expression of novel extracellular sulfatases Sulf-1 and Sulf-2 in normal and osteoarthritic articular cartilage. Arthritis Res Ther. 2008;10(3):R61.
27. Guilak F, Alexopoulos LG, Upton ML, Youn I, Choi JB, Cao L, et al. The pericellular matrix as a transducer of biomechanical and biochemical signals in articular cartilage. Ann N Y Acad Sci. 2006;1068:498–512.
28. Jenuwein T, Allis CD. Translating the histone code. Science. 2001;293(5532):1074–80.
29. Urnov FD. Chromatin remodeling as a guide to transcriptional regulatory networks in mammals. J Cell Biochem. 2003;88(4):684–94.
30. Kruh J. Effects of sodium butyrate, a new pharmacological agent, on cells in culture. Mol Cell Biochem. 1982;42(2):65–82.
31. Chang S, Pikaard CS. Transcript profiling in Arabidopsis reveals complex responses to global inhibition of DNA methylation and histone deacetylation. J Biol Chem. 2005;280(1):796–804.
32. Reid G, Metivier R, Lin CY, Denger S, Ibberson D, Ivacevic T, et al. Multiple mechanisms induce transcriptional silencing of a subset of genes, including oestrogen receptor alpha, in response to deacetylase inhibition by valproic acid and trichostatin A. Oncogene. 2005;24(31):4894–907.
33. Nawaz Z, Baniahmad C, Burris TP, Stillman DJ, O'Malley BW, Tsai MJ. The yeast SIN3 gene product negatively regulates the activity of the human progesterone receptor and positively regulates the activities of GAL4 and the HAP1 activator. Mol Gen Genet. 1994;245(6):724–33.
34. Mariadason JM, Corner GA, Augenlicht LH. Genetic reprogramming in pathways of colonic cell maturation induced by short chain fatty acids: comparison with trichostatin A, sulindac,

and curcumin and implications for chemoprevention of colon cancer. Cancer Res. 2000;60(16):4561–72.
35. Chambers AE, Banerjee S, Chaplin T, Dunne J, Debernardi S, Joel SP, et al. Histone acetylation-mediated regulation of genes in leukaemic cells. Eur J Cancer. 2003;39(8):1165–75.
36. Libby P, Aikawa M. New insights into plaque stabilisation by lipid lowering. Drugs. 1998;56(suppl 1):9–13. (discussion 33).
37. McCawley LJ, Matrisian LM. Matrix metalloproteinases: multifunctional contributors to tumor progression. Mol Med Today. 2000;6(4):149–56.
38. Mitchell PG, Magna HA, Reeves LM, Lopresti-Morrow LL, Yocum SA, Rosner PJ, et al. Cloning, expression, and type II collagenolytic activity of matrix metalloproteinase-13 from human osteoarthritic cartilage. J Clin Invest. 1996;97(3):761–8.
39. Verdin E, Dequiedt F, Kasler HG. Class II histone deacetylases: versatile regulators. Trends Genet. 2003;19(5):286–93.
40. Chang S, Young BD, Li S, Qi X, Richardson JA, Olson EN. Histone deacetylase 7 maintains vascular integrity by repressing matrix metalloproteinase 10. Cell. 2006;126(2):321–34.
41. Jensen ED, Schroeder TM, Bailey J, Gopalakrishnan R, Westendorf JJ. Histone deacetylase 7 associates with Runx2 and represses its activity during osteoblast maturation in a deacetylation-independent manner. J Bone Miner Res. 2008;23(3):361–72.
42. Mengshol JA, Vincenti MP, Brinckerhoff CE. IL-1 induces collagenase-3 (MMP-13) promoter activity in stably transfected chondrocytic cells: requirement for Runx-2 and activation by p38 MAPK and JNK pathways. Nucleic Acids Res. 2001;29(21):4361–72.
43. Wang X, Manner PA, Horner A, Shum L, Tuan RS, Nuckolls GH. Regulation of MMP-13 expression by RUNX2 and FGF2 in osteoarthritic cartilage. Osteoarthr Cartil. 2004;12(12):963–73.
44. Kawaguchi H. Endochondral ossification signals in cartilage degradation during osteoarthritis progression in experimental mouse models. Mol Cells. 2008;25(1):1–6.
45. Kamekura S, Kawasaki Y, Hoshi K, Shimoaka T, Chikuda H, Maruyama Z, et al. Contribution of runt-related transcription factor 2 to the pathogenesis of osteoarthritis in mice after induction of knee joint instability. Arthritis Rheum. 2006;54(8):2462–70.
46. Venter JC, Adams MD, Myers EW, Li PW, Mural RJ, Sutton GG, et al. The sequence of the human genome. Science. 2001;291(5507):1304–51.
47. Iliopoulos D, Malizos KN, Tsezou A. Epigenetic regulation of leptin affects MMP-13 expression in osteoarthritic chondrocytes: possible molecular target for osteoarthritis therapeutic intervention. Ann Rheum Dis. 2007;66(12):1616–21.
48. Yun K, Im SH. Transcriptional regulation of MMP13 by Lef1 in chondrocytes. Biochem Biophys Res Commun. 2007;364(4):b1009–14.
49. Mengshol JA, Vincenti MP, Coon CI, Barchowsky A, Brinckerhoff CE. Interleukin-1 induction of collagenase 3 (matrix metalloproteinase 13) gene expression in chondrocytes requires p38, c-Jun N-terminal kinase, and nuclear factor kappaB: differential regulation of collagenase 1 and collagenase 3. Arthritis Rheum. 2000;43(4):801–11.
50. Brenner DA, O'Hara M, Angel P, Chojkier M, Karin M. Prolonged activation of jun and collagenase genes by tumour necrosis factor-alpha. Nature. 1989;337(6208):661–3.
51. Conca W, Kaplan PB, Krane SM. Increases in levels of procollagenase messenger RNA in cultured fibroblasts induced by human recombinant interleukin 1 beta or serum follow c-jun expression and are dependent on new protein synthesis. J Clin Invest. 1989;83(5):1753–7.
52. Borden P, Solymar D, Sucharczuk A, Lindman B, Cannon P, Heller RA. Cytokine control of interstitial collagenase and collagenase-3 gene expression in human chondrocytes. J Biol Chem. 1996;271(38):23577–81.
53. Baker AH, Edwards DR, Murphy G. Metalloproteinase inhibitors: biological actions and therapeutic opportunities. J Cell Sci. 2002;115(Pt 19):3719–27.

MicroRNA-140 plays dual roles in both cartilage development and homeostasis

Shigeru Miyaki, Tempei Sato, Atsushi Inoue, et al.

Genes Dev. 2010 24: 1173-1185 originally published online May 13, 2010
Access the most recent version at doi:10.1101/gad.1915510

MicroRNA-140 plays dual roles in both cartilage development and homeostasis

Shigeru Miyaki,[1,4] Tempei Sato,[2,4] Atsushi Inoue,[2] Shuhei Otsuki,[1] Yoshiaki Ito,[2] Shigetoshi Yokoyama,[2] Yoshio Kato,[3] Fuko Takemoto,[2] Tomoyuki Nakasa,[2] Satoshi Yamashita,[2] Shuji Takada,[2] Martin K. Lotz,[1] Hiroe Ueno-Kudo,[2] and Hiroshi Asahara[1,2,5]

[1]Department of Molecular and Experimental Medicine, The Scripps Research Institute, La Jolla, California 92037, USA; [2]Department of Systems Biomedicine, National Research Institute for Child Health and Development, Tokyo 157-8535, Japan; [3]Biomedical Research Institute for Cell Engineering (RICE), National Institute of Advanced Industrial Science and Technology (AIST), Tsukuba 305-8562, Japan

Osteoarthritis (OA), the most prevalent aging-related joint disease, is characterized by insufficient extracellular matrix synthesis and articular cartilage degradation, mediated by several proteinases, including Adamts-5. miR-140 is one of a very limited number of noncoding microRNAs (miRNAs) specifically expressed in cartilage; however, its role in development and/or tissue maintenance is largely uncharacterized. To examine miR-140 function in tissue development and homeostasis, we generated a mouse line through a targeted deletion of miR-140. miR-140$^{-/-}$ mice manifested a mild skeletal phenotype with a short stature, although the structure of the articular joint cartilage appeared grossly normal in 1-mo-old miR-140$^{-/-}$ mice. Interestingly, miR-140$^{-/-}$ mice showed age-related OA-like changes characterized by proteoglycan loss and fibrillation of articular cartilage. Conversely, transgenic (TG) mice overexpressing miR-140 in cartilage were resistant to antigen-induced arthritis. OA-like changes in miR-140-deficient mice can be attributed, in part, to elevated *Adamts-5* expression, regulated directly by miR-140. We show that miR-140 regulates cartilage development and homeostasis, and its loss contributes to the development of age-related OA-like changes.

[*Keywords*: MicroRNA; miR-140; osteoarthritis; cartilage; *Adamts-5*]

Supplemental material is available at http://www.genesdev.org.

Received February 10, 2010; revised version accepted April 13, 2010.

MicroRNAs (miRNAs) are a class of noncoding RNAs that negatively regulate genes involved in numerous biological processes. Hundreds of miRNAs have been identified in various organisms, and many are evolutionarily conserved. Moreover, an estimated one-third of all mammalian mRNAs are regulated by miRNAs, demonstrating the essential role of miRNAs in controlling gene expression (Lewis et al. 2005). miRNAs are generated as long primary transcripts (pri-miRNAs) that are processed by the enzymes Drosha and Dicer into short ribonucleotides (~22 nucleotides long). The mature miRNAs are then incorporated into the RNA-induced silencing complex (RISC). The miRNA–RISC complex mediates the degradation of specific mRNA targets and/or the repression of mRNA translation via interactions with the 3′ untranslated regions (UTRs) that are partially sequence-specific (Bartel 2004). Several miRNAs exhibit a tissue-specific or developmental stage-specific expression pattern and have been associated with human diseases such as heart disease (van Rooij et al. 2006) and arthritis (Iliopoulos et al. 2008; Nakasa et al. 2008; Stanczyk et al. 2008; Yamasaki et al. 2009). In addition, mice with limb- or cartilage-specific deletion of the miRNA-processing enzyme Dicer exhibited a severe phenotype with reduced limb size but normal patterning (Harfe et al. 2005; Kobayashi et al. 2008). Dicer is indispensable for mature, functional miRNAs; therefore, this finding suggests that miRNAs play a critical role in skeletal development.

Recent studies have revealed the cartilage-specific expression of miR-140 in mouse embryos and zebrafish (Wienholds et al. 2005; Tuddenham et al. 2006). Using an miRNA microarray, we demonstrated considerable miRNA expression differences between human articular chondrocytes and mesenchymal stem cells. Furthermore, miR-140 exhibited the largest expression difference between the two cell types (Miyaki et al. 2009). The study of miR-140 may thus be the key miRNA to open a new insight of cartilage biology. However, the function of miRNAs in articular cartilage has not been analyzed by targeted deletion.

Previous studies also found reduced miR-140 expression in human osteoarthritis (OA) cartilage (Iliopoulos

[4]These authors contributed equally to this work.
[5]Corresponding author.
E-MAIL asahara@scripps.edu; FAX (858) 784-2695.
Article published online ahead of print. Article and publication date are online at http://www.genesdev.org/cgi/doi/10.1101/gad.1915510.

et al. 2008; Miyaki et al. 2009), which may contribute to the abnormal gene expression pattern characteristic of OA. These findings prompted us to examine the role of miR-140 in cartilage development and homeostasis by generating miR-140-deficient mice and cartilage-specific miR-140 transgenic (TG) mice. The results indicate that miR-140 plays dual roles in both cartilage development and homeostasis, in part via regulating *Adamts-5*, a major cartilage matrix-degrading protease in OA (Glasson et al. 2005; Stanton et al. 2005).

Results

Targeted deletion of cartilage-specific miR-140

To define the in vivo function of miR-140, we targeted the mouse miR-140 sequence for deletion. We deleted the region containing miR-140 in the intron between exons 16 and 17 of the WW domain-containing E3 ubiquitin protein ligase 2 (Wwp2), and inserted a neomycin (neo) resistance cassette flanked by loxP sites (Fig. 1A,B). The floxed phosphoglycerine kinase (PGK)-neo cassette was removed by crossing with Meox-Cre TG mice, and Cre-mediated neo excision was confirmed by genomic PCR (Fig. 1C). Quantitative real-time PCR (qPCR) analysis of chondrocyte RNA showed a complete absence of miR-140 in miR-140$^{-/-}$ mice (Fig. 1D). We confirmed that the Wwp2 protein levels were unchanged in miR-140$^{-/-}$ mice (Fig. 1E).

Skeletal growth in miR-140$^{-/-}$ mice

miR-140$^{-/-}$ mice were born in normal Mendelian ratios and were fertile. Skeletal development during embryogenesis in miR-140$^{-/-}$ mice appeared grossly normal (Fig. 2A). Postnatally, miR-140$^{-/-}$ mice manifested a mild skeletal phenotype, with short stature and low body weight (Fig. 2B–D), as well as craniofacial deformities characterized by a short snout and domed skull (Fig. 2E). This craniofacial phenotype in miR-140$^{-/-}$ mice shows partial similarity to that of cartilage-specific Dicer-deficient mice (Kobayashi et al. 2008), supporting the notion that miR-140 is a tissue-specific miRNA important in cartilage development. As miR-140 is expressed in cartilage and not in other tissues by whole-mount in situ hybridization (Wienholds et al. 2005; Tuddenham et al. 2006), reduced skeletal tissues of miR-140$^{-/-}$ mice may account for this weight loss phenotype.

The hind-limb bones were shorter in miR-140$^{-/-}$ mice compared with wild-type mice (Fig. 3A). In the growth plates of wild-type mice, miR-140 was expressed in proliferating chondrocytes but not in hypertrophic chondrocytes that expressed *Col10a1* (Fig. 3B). The width of the tibial growth plates in 1-mo-old mice was reduced in miR-140$^{-/-}$ mice compared with wild-type mice (Fig. 3C). The number of proliferating chondrocytes was significantly decreased at postnatal day 10 (P10) in miR-140$^{-/-}$ mouse growth plates (Fig. 3D,E), whereas no significant changes were observed in hypertorophyic zones (Fig. 3C). These findings indicate that the mild skeletal phenotype in miR-140$^{-/-}$ mice with short stature results from a reduction in proliferating chondrocytes.

OA-like pathology in miR-140$^{-/-}$ mouse knee joints

Chondrocytes play a critical role not only in skeletal development, but also in articular cartilage formation and maintenance. Analysis of pri-miR-140 expression in 2-mo-old wild-type mice by in situ hybridization showed miR-140 expression in chondrocytes from the surface to middle zones of articular cartilage and in the menisci, overlapping with expression of the chondrocyte marker *Col2a1* (Fig. 4A). Furthermore, the structure and shape of knee joints—including articular cartilage, menisci, and ligaments—were analyzed by Safranin O staining and three-dimensional (3D) computed tomography (CT). They all appeared to be normal in miR-140$^{-/-}$ mice at birth and 1 mo of age (Supplemental Fig. S1).

Because miR-140 expression was shown to be reduced in human OA cartilage (Iliopoulos et al. 2008; Miyaki et al. 2009), we examined the potential role of miR-140 in cartilage homeostasis. OA initiation and progression is mediated by various stimuli and circumstances, including the following three main factors: age-related changes in homeostatic balance, excessive mechanical stress sometimes triggered by joint injury, and transient inflammation in the articular joint damaging the cartilage matrix. Therefore, to determine the potential role of miR-140 in cartilage homeostasis, we used three different animal models of OA: an aging model, a surgical model, and an antigen-induced arthritis (AIA) model.

First, we tested whether loss of miR-140 affected age-related onset of OA changes, and observed that miR-140$^{-/-}$ mice developed an age-related OA-like pathology. Knee joints from 3-mo-old mice showed reduced Safranin O staining in femoral condyles and tibial plateaus, indicative of proteoglycan loss (Fig. 4B). By 8 mo, overt cartilage degradation was apparent as more severe proteoglycan loss, a roughened articular surface, and fibrillation; these changes were not observed in age-matched wild-type mice (Fig. 4B). By 12 mo, miR-140$^{-/-}$ mice showed severe structural cartilage defects (Fig. 4B) that were not associated with synovial hyperplasia. We also observed OA-like changes in elbow and ankle joint articular cartilage of miR-140$^{-/-}$ mice at 12 mo old, compared with articular cartilage from wild-type mice (Supplemental Fig. S2). To quantify OA-like pathological changes in the articular cartilage, an OA scoring system was used to validate several aspects of the histological changes (Chambers et al. 2001; Glasson et al. 2004). OA scores were significantly higher in miR-140$^{-/-}$ mice compared with wild-type mice (Fig. 4C). These results support the hypothesis that miR-140 is a critical regulator of cartilage homeostasis, and its loss contributes to cartilage degradation characteristic of OA.

Next, we used the surgical arthritis model, in which the articular cartilage was exposed to an excessive mechanical load, due to joint instability caused by surgical resection of the medial meniscotibial ligament (MMTL) (Glasson et al. 2007). Consistent with observations in the aging OA model, the surgical arthritis model also demonstrated

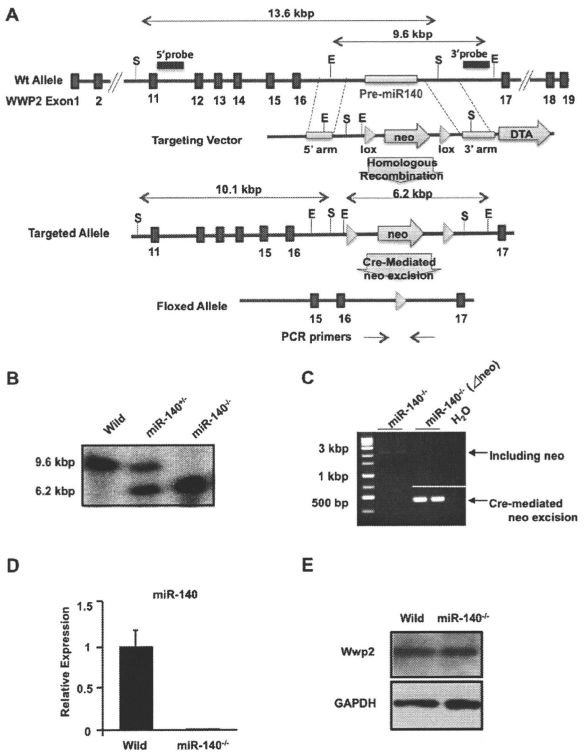

Figure 1. Generation of miR-140-null mice. (*A*) Targeting of miR-140. The targeting vector was constructed to replace the endogenous pri-miR-140 locus with a PGK-neo cassette by homologous recombination. The 5′ probe and 3′ probe used for Southern blot and PCR primers used for genotyping are indicated. (E) EcoRV, (S) SphI. (*B*) Southern blot analysis of wild-type (Wild) and miR-140 mutant mice. Genomic DNA was digested with EcoRV and probed with the indicated 3′ probe. (*C*) Confirmation of Cre-mediated neo excision by genomic PCR. The floxed PGK-neo cassette was removed by crossing with Meox-Cre TG mice. (*D*) Expression of mature miR-140 in wild-type (Wild) and miR-140$^{-/-}$ mouse embryos at E11.5 as assessed by qPCR. Mature miR-140 was not detected in miR-140$^{-/-}$ mice. Data are expressed as mean ± SEM ($n = 3$). (*E*) Western blot analysis of Wwp2. Wwp2 expression was not detectably different in miR-140$^{-/-}$ compared with wild-type mice.

that miR-140$^{-/-}$ mice exhibit accelerated proteoglycan loss and fibrillation of articular cartilage in knee joints compared with the wild-type mice at 8 wk after surgery, which is reflected in higher OA scores (Fig. 4D,E).

Cartilage-specific miR-140 TG mice exhibited resistance to AIA

We further examined the role of miR-140 in articular cartilage by using the AIA model, in which transient inflammation was induced by antigen injection. Inflammatory signals such as interleukin-1β (IL-1β) from the chondrocytes and synovial membrane of articular joint spaces mediate OA progression, in part by up-regulating the expression of cartilage matrix degradation enzymes in chondrocytes (Goldring and Goldring 2007). In this model, as well as in human OA pathogenesis, transient joint inflammation causes cartilage damage by the induction of cartilage-degrading enzymes. The AIA model is advantageous in that it leads to cartilage damage in a

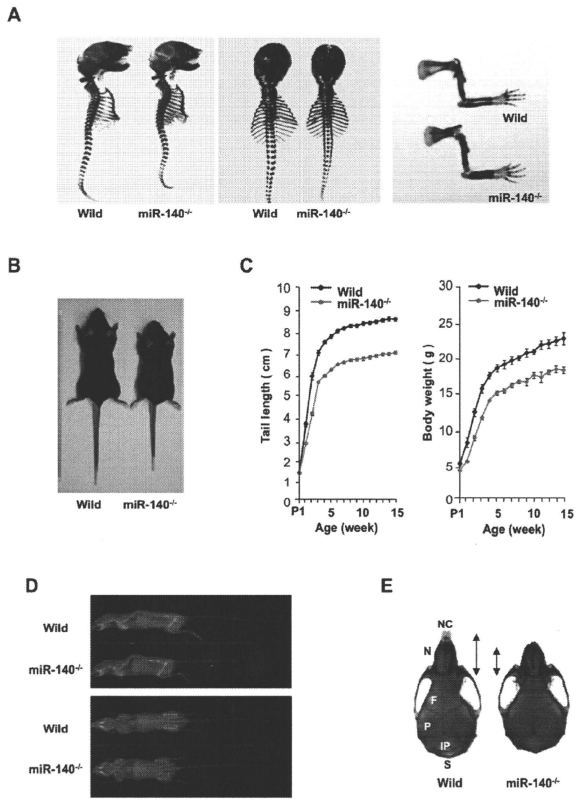

Figure 2. Growth retardation in *miR-140*$^{-/-}$ mice. (*A*) Skeletal preparation with Alcian blue/Alizarin red staining of wild-type (Wild) and miR-140$^{-/-}$ littermates at E17.5. miR-140$^{-/-}$ embryos exhibited no overt abnormalities in skeletal development. (*Left*) Whole-mount.(*Middle*) Dorsal view. (*Right*) Forelimb. (*B*) Appearance of wild-type and miR-140$^{-/-}$ mice at 4 wk. Growth retardation was observed in miR-140$^{-/-}$ mice. (*C*) Wild-type and miR-140$^{-/-}$ mice were scored for tail length and body weight at various postnatal stages. miR-140$^{-/-}$ mice showed growth retardation 1 wk after birth (tail length, $P < 0.01$; body weight, $P < 0.05$). Data are expressed as mean ± SEM (n = 5–12). (*D*) No gross skeletal changes were detectable by X-ray in 3-mo-old mice. (*E*) Skulls of wild-type and miR-140$^{-/-}$ mice stained with Alcian blue/Alizarin red. Dorsal views are shown. miR-140$^{-/-}$ mice exhibited craniofacial bone defects characterized by short nasal bone, short maxilla, and domed skull. (NC) Nasal capsule, (N) nasal bone, (F) frontal bone, (P) parietal bone, (IP) interparietal bone, (S) supraoccipital bone.

short time in wild-type mice, which enables us to monitor the beneficial effects of miR-140 against cartilage degradation by a gain-of-function approach.

Accordingly, we generated cartilage-specific TG mice in which miR-140 expression was driven by a well-characterized *Col2a1* enhancer sequence (Fig. 5A; Zhou et al. 1995; Krebsbach et al. 1996). We obtained three lines of TG mice and observed up-regulation of miR-140 in cartilage of all three lines (Fig. 5B). These TG mice did not show any apparent abnormalities in skeletal development (data

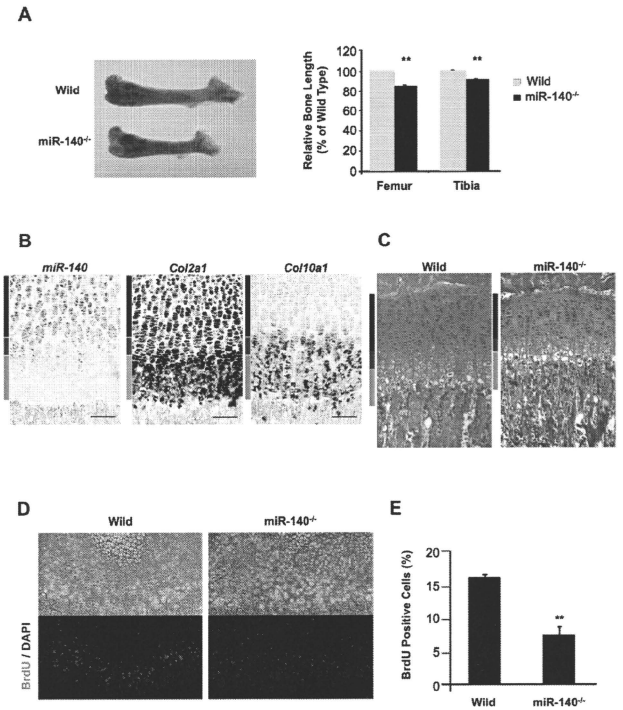

Figure 3. Skeletal growth in miR-140$^{-/-}$ mice. (*A*, *left*) Length of femur. (*Right*) Long bones were significantly shorter in the miR-140$^{-/-}$ mice. Data are expressed as mean ± SEM ($n = 3$). (**) $P < 0.01$. (*B*) Expression of *pri-miR-140*, *Col2a1*, and *Col10a1* in the tibial growth plates of P10 mice. miR-140 was detected in proliferating chondrocytes. (Blue bar) Proliferative zone, (red bar) prehypertrophic zone, (green bar) hypertrophic zone. (*C*) Safranin O staining of the tibial growth plates in 1-mo-old mice. The proliferating zone was reduced in miR-140$^{-/-}$ mice compared with wild-type mice (Wild). (*D*,*E*) BrdU-positive cells were significantly reduced in miR-140$^{-/-}$ mice at P10. BrdU (green) and DAPI (blue) staining indicate nuclei. Data are expressed as mean ± SEM ($n = 3$). (**) $P < 0.01$.

not shown). To examine whether the miR-140 level in articular chondrocytes affects cartilage sensitivity to experimental challenge, we assessed AIA in knee joints of miR-140 TG mice, miR-140$^{-/-}$ mice, and wild-type mice. We observed similar levels of synovial hyperplasia among miR-140 TG mice, miR-140$^{-/-}$ mice, and wild-type mice; however, miR-140$^{-/-}$ mice showed reduced Safranin O staining (Fig. 5C). Importantly, miR-140 TG mice were resistant to proteoglycan and type II collagen loss compared with wild-type mice. To quantify the extent of matrix degradation, we used the Mankin scoring system (Mankin 1971; Zemmyo et al. 2003) for proteoglycan loss. Mankin scores were significantly lower in miR-140 TG mice and significantly higher in miR-140$^{-/-}$ mice compared with wild-type mice (Fig. 5D). These findings are consistent with the idea that miR-140 protects against OA progression.

ADAMTS-5 is a direct target of miR-140 and mediates OA pathogenesis

Identification of miR-140 target genes can provide new insights into miR-140 function and OA pathogenesis. To achieve this goal, we applied DNA array analysis to identify miRNA targets (Lim et al. 2005; Valencia-Sanchez et al. 2006). Based on computationally predicted target

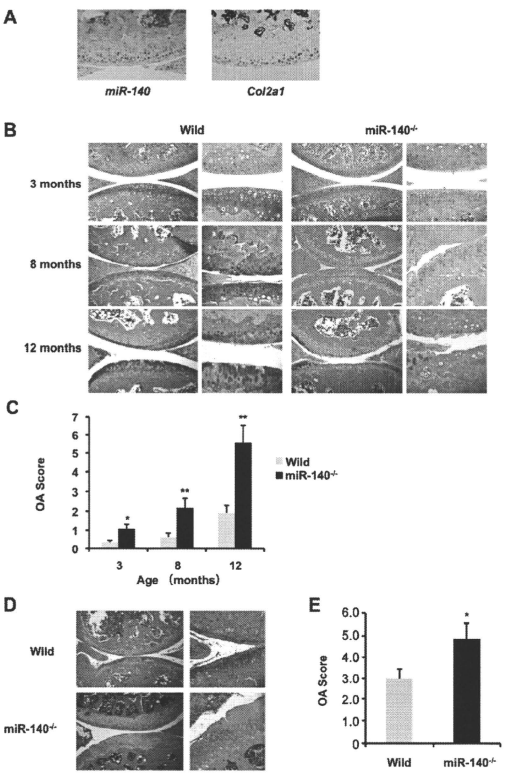

Figure 4. miR-140$^{-/-}$ mice exhibit OA-like pathology. (*A*) Expression of *pri-miR-140* (*left*) and *Col2a1* (*right*) in articular cartilage of the knee joints in 2-mo-old mice. miR-140 was detected in chondrocytes from the surface to middle zones of articular cartilage. (*B*) Safranin O staining of the knee joint in 3-mo-old mice (wild-type, $n = 6$; miR-140$^{-/-}$, $n = 6$), 8-mo-old mice (wild-type, $n = 15$; miR-140$^{-/-}$, $n = 13$), and 12-mo-old mice (wild-type, $n = 12$; miR-140$^{-/-}$, $n = 11$). miR-140 deletion caused an early onset of OA-like changes. (*C*) Histopathologic scores of knee joints. OA scores were significantly increased in miR-140$^{-/-}$ mice. Data are expressed as mean ± SEM. (*) $P < 0.05$; (**) $P < 0.01$. (*D*) Surgical OA was induced in 10-wk-old wild-type and miR-140$^{-/-}$ mice by resecting the MMTL (wild-type mice, $n = 8$; miR-140$^{-/-}$ mice, $n = 11$). The knee joints were harvested 8 wk after surgery and stained with Safranin O for histopathologic analysis. (*E*) miR-140$^{-/-}$ mice showed significantly increased OA scores compared with wild-type mice after surgery. Data are expressed as mean ± SEM. (*) $P < 0.05$.

genes found in the online database TargetScan (http://www.targetscan.org), 17 of the mRNAs in the array that were increased in miR-140$^{-/-}$ chondrocytes exhibited conserved miR-140-binding sites in their 3′ UTRs with 7-mer or 8-mer seeds (Supplemental Table S1). Among the most overexpressed was the gene for ADAMTS-5, which degrades aggrecan and is a critical enzyme for OA pathogenesis (Glasson et al. 2005; Stanton et al. 2005). We analyzed *Adamts-5* sequences in humans, mice, rats, and dogs and observed highly conserved miR-140-binding sites with 8-mer seeds in the *Adamts-5* 3′ UTR (Fig. 6A). *Adamts-5* expression was significantly increased in chondrocytes from miR-140$^{-/-}$ mice and significantly decreased in those from miR-140 TG mice compared with wild-type (Fig. 6B). Similarly, increased ADAMTS-5 protein expression in articular cartilage in miR-140$^{-/-}$ mice at 1 and 3 mo old was visualized by immunohistochemistry (Fig. 6C,D; Supplemental Fig. S3). To confirm that miR-140 plays a critical role in aggrecanolysis, we quantified proteoglycan loss from cartilage in wild-type mice, miR-140 TG mice, and miR-140$^{-/-}$ mice. Femoral head cartilage explants were cultured with or without IL-1β, which is a potent catabolic stimulus of cartilage matrix degradation. Cartilage explants from miR-140$^{-/-}$ mice showed significantly increased proteoglycan release compared with wild-type cartilage (Fig. 6E). In contrast, IL-1β-induced proteoglycan release from the cartilage of miR-140 TG mice was significantly lower compared with wild-type cartilage.

We further tested whether miR-140 regulates *Adamts-5* mRNA in chondrocytes. Treatment of chondrocytes from

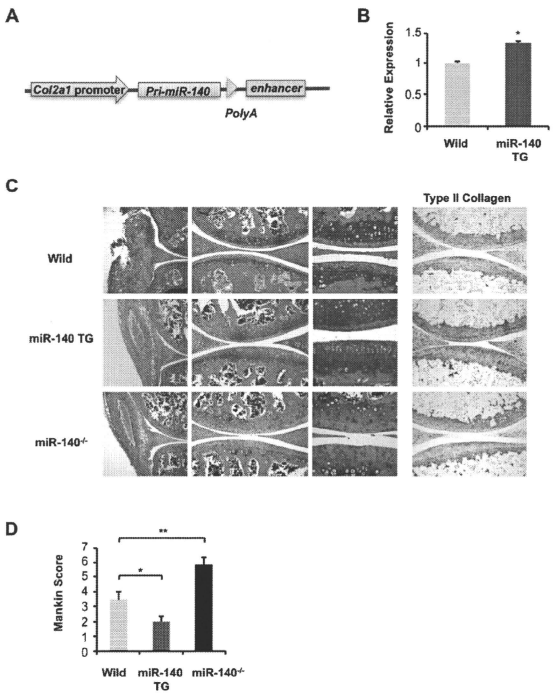

Figure 5. Cartilage-specific miR-140 TG mice are resistant to AIA. (*A*) miR-140 TG mice were generated with a construct using the cartilage-specific *Col2a1* promoter. (*B*) Significantly increased expression of miR-140 in chondrocytes of miR-140 TG mice compared with those of wild-type mice was confirmed by qPCR analysis. These data are results from representatives of a single mouse line ($n = 3$). Data are expressed as mean ± SEM. (*) $P < 0.05$. (*C*) Seven days after induction of AIA, Safranin O staining and immunohistochemistry for type II collagen shows higher proteoglycan and collagen levels in miR-140 TG mice and lower levels in miR-140$^{-/-}$ mice compared with wild type. (*D*) Mankin score for proteoglycan loss in wild-type mice ($n = 5$), miR-140 TG mice ($n = 6$), and miR-140$^{-/-}$ mice ($n = 6$) 7 d after induction of AIA. Data are expressed as mean ± SEM. (*) $P < 0.05$; (**) $P < 0.01$.

miR-140$^{-/-}$ mice with ds-miR-140 reduced *Adamts-5* expression (Fig. 6F), supporting the notion that miR-140 negatively regulates *Adamts-5* mRNA. To determine whether *Adamts-5* is a direct miR-140 target in intact cells, the Adamts-5 3′ UTR, which includes a putative miR-140-binding site, was cloned downstream from the luciferase gene in an expression vector driven by the SV-40 promoter (*Adamts-5* 3′ UTR). Cotransfection of HEK293T cells with ds-miR-140 significantly reduced luciferase activity in cells transfected with *Adamts-5* 3′ UTR (Fig. 6G). No changes in luciferase activity were observed in cells transfected with the mutated luciferase expression vector (*Adamts-5* mut 3′ UTR) in response to ds-miR-140 (Fig. 6G). Taken together, these data indicate that miR-140 directly regulates *Adamts-5* expression and proteoglycan loss in articular cartilage.

Discussion

Recent studies have revealed that miRNAs play critical roles in various biological events, including development, disease, and immunity (Stefani and Slack 2008; Xiao and Rajewsky 2009). However, few molecular networks regulated by miRNAs have been characterized in detail, due in part to difficulty in determining the direct targets of each miRNA. Tissue-specific miRNAs targeting mice have

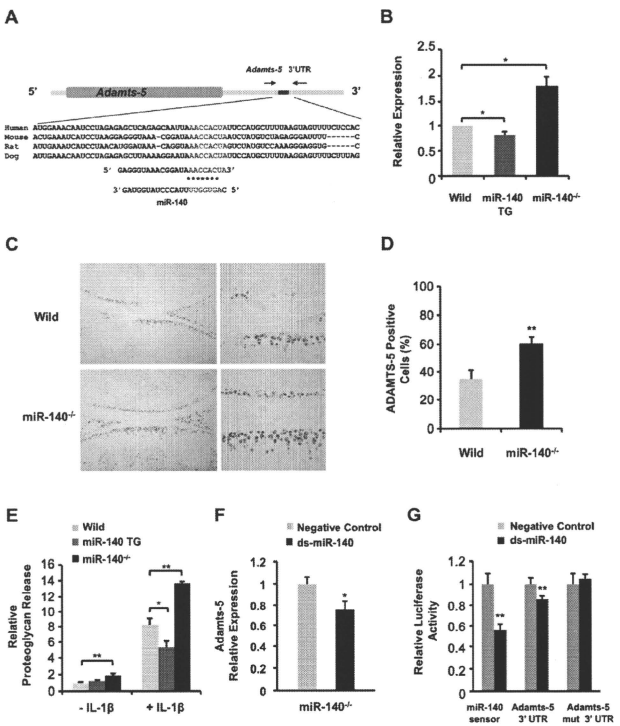

Figure 6. miR-140 regulates *Adamts-5* expression. (*A*) miR-140 targets the *Adamts-5* 3′ UTR. Sequence alignment of a putative miR-140-binding site in the *Adamts-5* 3′ UTR shows a high level of sequence conservation and complementarity with miR-140. (*B*) Differential *Adamts-5* expression in rib chondrocytes from wild-type mice, miR-140 TG mice, and miR-140$^{-/-}$ mice was evaluated by qPCR. Data are expressed as fold differences compared with wild-type chondrocytes (mean ± SEM; n = 4–5 per genotype). (*) $P < 0.05$. (*C*) Histologic analysis of articular cartilage from 3-mo-old mice. Immunostaining showed an increase in ADAMTS-5-positive chondrocytes in miR-140$^{-/-}$ mice. (*D*) ADAMTS-5-positive cells were detected in wild-type and miR-140$^{-/-}$ cartilage. Knee joints from 3-mo-old wild-type (n = 3) and miR-140$^{-/-}$ (n = 3) mice were examined. Data are expressed as mean ± SEM. (**) $P < 0.01$. (*E*) Femoral head cartilage explants from miR-140$^{-/-}$ mice cultured in DMEM only (n = 13) or DMEM containing IL-1β (n = 6) showed significantly increased proteoglycan release compared with wild-type mice in DMEM only (n = 17) or DMEM containing IL-1β (n = 6). IL-1β-induced proteoglycan release in miR-140 TG mice in medium (n = 12) was significantly lower compared with that of wild-type mice (n = 10). Data are expressed as fold differences compared with wild-type explants in DMEM only (mean ± SEM). (*) $P < 0.05$; (**) $P < 0.01$. (*F*) Relative *Adamts-5* expression in miR-140$^{-/-}$ chondrocytes was determined by qPCR after transfection with ds-miR-140 (black). Data are expressed as fold differences relative to negative control cells (gray, mean ± SEM). (*) $P < 0.05$. (*G*) Luciferase activity of pLuc2-miR-140 sensor (miR-140 sensor), pLuc2-*Adamts-5* 3′ UTR (*Adamts-5* 3′ UTR), and pLuc2-*Adamts-5* 3′ UTR with mutated miR-140-binding site (*Adamts-5* mut 3′ UTR). Luciferase activity was determined in HEK293T cells transfected with miR-140 sensor, *Adamts-5* 3′ UTR, or *Adamts-5* mut 3′ UTR along with a ds-miR-140 (black) or negative control miRNA (gray) (n = 6). Data are expressed as relative luciferase activity (mean ± SEM). (*) $P < 0.05$; (**) $P < 0.01$.

been generated to elucidate the role of miRNAs in tissue and organ development, including heart and muscles (van Rooij et al. 2007; Zhao et al. 2007; Liu et al. 2008); however, so far there is very limited information on the function of miRNAs in cartilage/bone development and related diseases.

Transcription factor SRY-box-containing gene 9 (Sox9) is a master regulator of chondrocyte differentiation (de Crombrugghe et al. 2000). The expression of miR-140 shadows *Sox9* expression, and the deletion of Sox9 diminishes miR-140 expression during embryogenesis (S Miyaki and H Asahara, unpubl.), indicating that miR-140 is under Sox9 regulation in chondrocytes. Although the disruption of Sox9 in mice results in a complete lack of cartilage development, miR-140$^{-/-}$ mice showed only a mild skeletal phenotype, with short stature and craniofacial changes. Results of studies targeting mice at specific developmental stages show that Sox9 is not only essential for chondrogenesis initiation, but is also important to produce large numbers of proliferating chondrocytes (Akiyama 2008). In the present study, the expression pattern of miR-140 was detected in the proliferation zone during endochondral ossification, and fewer proliferating chondrocytes were observed in miR-140$^{-/-}$ mice. Thus, regulation of proliferating chondrocytes may be one of the Sox9 functions mediated by miR-140.

Mice that are Dicer-deficient in cartilage tissues show a progressive and profound reduction in proliferating growth plate chondrocytes, which leads to severe skeletal growth defects and premature death (Kobayashi et al. 2008); however, this severe phenotype may reflect the effect of reducing all miRNAs, including ubiquitous ones. In this regard, our study provides the first example showing bone and cartilage phenotypes in mice caused by tissue-specific miRNA.

The phenotype of miR-140$^{-/-}$ mice on skeletal framework is not drastic, and the mice can survive for >1 yr; however, this mild phenotype provides us with an opportunity to monitor another aspect of miR-140 function in cartilage. Chondrocytes have two major functions: endochondral ossification for proper skeletal development, and articular cartilage maintenance for joint movement. Although chondrocytes in endochondral ossification disappear after bone development has been completed, articular cartilage chondrocytes persist, secreting the extracellular matrix that protects tissue from damage. The role of miRNAs in tissue homeostasis has not yet been well elucidated, other than a few studies such as those reporting the critical role of miR-143/145 in smooth muscle cell maintenance (Elia et al. 2009).

Articular cartilage is a good tissue for characterizing the molecular network involved in tissue homeostasis. The cartilage framework consists of a cartilage-specific extracellular matrix, which includes type II collagen and proteoglycans, and is maintained by chondrocytes embedded in the matrix. To maintain the integrity of this cartilage framework, the matrix is continuously undergoing remodeling via matrix-degrading enzymes; this degradation is balanced by the secretion of newly synthesized matrix proteins. The balance of these catabolic and anabolic signals in cartilage tissue is critical for cartilage homeostasis; aging, inflammation, or injuries may promote catabolic signals, including ADAMTS-5 and matrix metallopeptidase-13 (MMP-13), which can lead to arthritis changes. OA is the result of this age-related loss of the homeostatic balance between cartilage degradation and repair; it is aggravated by joint inflammation or excessive mechanical load (Goldring and Goldring 2007; Hashimoto et al. 2008; Goldring and Marcu 2009). Treatment options are limited, and new therapeutic targets that regulate the cartilage homeostasis balance should be sought.

To determine the role of miR-140 in articular cartilage, we examined three different arthritis models: age-related, surgical, and inflammatory (AIA). Disruption of miR-140 in vivo induced the early onset of spontaneous OA-like changes in articular cartilage of the age-related model and more severe OA-like changes in the surgical model. Transfection of human chondrocytes with ds-miR-140 down-regulated IL-1β-induced Adamts-5 expression (Miyaki et al. 2009). Consistent with our findings that miR-140 exerts a protective effect in cartilage, miR-140 TG mice were resistant to cartilage matrix degradation in the inflammatory model, suggesting that the regulation of miR-140 has important implications for drug design in OA treatment.

To address the mechanism of enhanced cartilage degradation in miR-140$^{-/-}$ mice, we showed the up-regulation of *Adamts-5*, a direct target of miR-140. ADAMTS-5 was shown to be a critical cartilage-degrading enzyme, because animals deficient in ADAMTS-5 activity are resistant to cartilage degeneration in the surgical OA model and inflammatory arthritis model (Glasson et al. 2005; Stanton et al. 2005). ADAMTS-5 also appears to be the major enzyme responsible for aggrecan degradation in human OA on the basis of increased mRNA and protein expression in OA cartilage (Malfait et al. 2002). Nevertheless, regulatory mechanisms of *Adamts-5* expression have not been clearly elucidated. Two groups reported recently that Runx2 regulates *Adamts-5* expression (Thirunavukkarasu et al. 2007), and hedgehog signaling regulates the expression of *Adamts-5* via Runx2 (Lin et al. 2009). In addition to these transcriptional regulations, in the present study we demonstrated that *Adamts-5* expression was tightly regulated by miR-140 at the post-transcriptional level.

Although the critical role of miR-140 in cartilage maintenance may be explained largely by identifying *Adamts-5* as its direct target, miRNAs are believed to regulate multiple target mRNAs; therefore, the role of miR-140 in cartilage homeostasis may involve the regulation of additional genes, as listed in Supplemental Table S1. Accordingly, gene expression analysis by microarray and qPCR revealed an up-regulation of other cartilage-related catabolic factors, such as matrix degradation enzymes, and a down-regulation of cartilage matrix genes in chondrocytes of miR-140$^{-/-}$ mice as early as P3 (Supplemental Fig. S2). These results suggest that miR-140 may suppress pathways other than *Adamts-5* expression, thus regulating the overall balance of cartilage matrix synthesis and degradation. Histone deacetylase 4 (HDAC4), which inhibits hypertrophic differentiation of chondrocytes (Vega et al. 2004), is thought to be an miR-140 target gene (Tuddenham et al. 2006); however, we did not observe significant changes in HDAC4 mRNA or protein expression in the endochondral plate or articular cartilage in the present study. The miR-140$^{-/-}$ and miR-140 TG lines may be useful in identifying other targets associated with cartilage development and homeostasis.